blood

Prepublished online Dec 28, 2009;
doi:10.1182/blood-2009-10-246116

Perforin activates clathrin and dynamin-dependent endocytosis, which is required for plasma membrane repair and delivery of granzyme B for granzyme-mediated apoptosis

Jerome Thiery, Dennis Keefe, Saviz Saffarian, Denis Martinvalet, Michael Walch, Emmanuel Boucrot, Tomas Kirchhausen and Judy Lieberman

Blood (print ISSN 0006-4971, online ISSN 1528-0020), is published semimonthly by the American Society of Hematology, 1900 M St, NW, Suite 200, Washington DC 20036.

Perforin activates clathrin and dynamin-dependent endocytosis, which is required for plasma membrane repair and delivery of granzyme B for granzyme-mediated apoptosis

Jerome Thiery,[1,2] Dennis Keefe,[1,2] Saviz Saffarian,[1,3] Denis Martinvalet,[1,2] Michael Walch[1,2] Emmanuel Boucrot,[1,3] Tomas Kirchhausen,[1,3] and Judy Lieberman[1,2,*]

[1]Program in Cellular and Molecular Medicine, Children's Hospital and Immune Disease Institute, Boston, MA
[2]Department of Pediatrics, Harvard Medical School, Boston, MA
[3]Department of Cell Biology, Harvard Medical School, Boston, MA

*Corresponding author: Judy Lieberman, Immune Disease Institute, Harvard Medical School, Warren Alpert Building, 200 Longwood Avenue, Boston MA 02115; Tel: (617) 278-3106; Fax: (617) 278-3134; e-mail: lieberman@idi.harvard.edu

Running Title: Perforin activates endocytosis of granzymes

Keywords: perforin, granzyme, cytotoxicity, endocytosis, cytotoxic T lymphocyte

Category: Immunobiology

Abstract

Cytotoxic T lymphocytes and natural killer cells destroy target cells via the polarized exocytosis of lytic effector proteins, perforin and granzymes, into the immunological synapse. How these molecules enter target cells is not fully understood. It is debated whether granzymes enter via perforin pores formed at the plasma membrane or whether perforin and granzymes are first endocytosed and granzymes are then released from endosomes into the cytoplasm. We previously showed that perforin disruption of the plasma membrane induces a transient Ca^{2+} flux into the target cell that triggers a wounded membrane repair response in which lysosomes and endosomes donate their membranes to reseal the damaged membrane. Here we show that perforin activates clathrin- and dynamin-dependent endocytosis, which removes perforin and granzymes from the plasma membrane to early endosomes, preserving outer membrane integrity. Inhibiting clathrin or dynamin-dependent endocytosis shifts death by perforin and granzyme B from apoptosis to necrosis. Thus by activating endocytosis to preserve membrane integrity, perforin facilitates granzyme uptake and avoids the proinflammatory necrotic death of a membrane-damaged cell.

Introduction

Cytotoxic T lymphocytes (CTL) and natural killer (NK) cells eliminate virus-infected cells and tumors by releasing the contents of cytotoxic granules into the immunological synapse formed with the target cell.[1,2] The granule mediators of cell death, serine proteases known as granzymes (Gzm), are delivered into the target cell cytosol by the granule pore-forming protein perforin (PFN).[3,4] The ability of Gzms to induce target cell apoptotic death is entirely PFN dependent.[2] PFN-deficient mice are highly susceptible to viruses and carcinogen-induced neoplasia and spontaneously develop B-cell lymphomas. Human congenital defects that result in impaired PFN synthesis, function or dysregulated release lead to familial haemophagocytic lymphohistiocytosis, a disease associated with profound immunodeficiency.[5,6]

How PFN delivers Gzms into target cells is not fully understood.[7,8] Because PFN multimerizes in a Ca^{2+}-dependent manner in membranes to form pores, the original model was that Gzms enter target cells via plasma membrane pores formed by multimerized PFN.[9,10] An influx of Ca^{2+} into target cells treated with PFN or attacked by CTLs suggests that PFN does indeed form plasma membrane pores.[11] However, at PFN sublytic concentrations that mimic physiological conditions of apoptosis induction, the pores that form in the plasma membrane might be too small to allow Gzms to pass through. In fact, small dyes that ought to be able to pass through PFN-sized pores do not disseminate into the cytosol after PFN treatment.[11,12] Moreover, Gzms do not directly enter the cytoplasm, as they would if they entered via cell membrane pores, but concentrate first in EEA-1-staining endosomes.[11,13] Therefore an alternate model postulates that PFN functions at the endosomal membrane to release endocytosed Gzms.[11,13]

Although PFN greatly enhances cellular uptake of Gzms[11], a clear mechanism to explain the increased endocytosis of Gzms is lacking. The Ca^{2+} influx induced in cells treated with sublytic PFN is transient, lasting at most 5 minutes.[11] This suggests that PFN forms small pores in the plasma membrane, but they are rapidly removed or repaired. We previously showed that the PFN-mediated increase in intracellular Ca^{2+} triggers a stereotypic damaged-membrane response (called cellular “wound-healing”), where intracellular vesicles, including endosomes and lysosomes, are rapidly mobilized to donate their membranes to reseal the damaged plasma membrane.[11,14,15] This repair response helps preserve the integrity of the cell membrane and allows the targeted cell to avoid immediate necrosis and undergo the slower

process of programmed cell death.[16] Although the "wound-healing" response might facilitate membrane repair, it does not explain how PFN enhances Gzm uptake. However, a recent study showed that the bacterial pore-forming protein, streptolysin-O (SLO), which can substitute for PFN for intracellular delivery of Gzms, activates Ca^{2+}-dependent, but dynamin (Dyn)-independent, endocytosis of damaged membrane to facilitate membrane repair.[17] If endocytosis occurs as part of the plasma membrane repair response (which PFN also activates[11]), it might provide a mechanism for Gzm and PFN co-endocytosis in target cells.

The aim of this study was to investigate how PFN enhances GzmB uptake. For the first time we visualize PFN within target cells. We find that PFN activates clathrin and Dyn-dependent endocytosis to remove PFN from the plasma membrane and enhance GzmB uptake. Both PFN and GzmB are endocytosed into giant EEA-1+ endosomes which form after PFN treatment. When endocytosis is inhibited, sublytic PFN or SLO become lytic, causing necrosis. Consequently inhibiting clathrin or Dyn pathways shifts the balance of target cell death by GzmB and PFN from apoptosis to necrosis. Our results suggest that the rapid induction of endocytosis to remove damaged cell membrane is an important component of the "wound-healing" response used by cytotoxic cells to induce apoptosis.

Materials and methods

(Additional methods can be found in supplementary online material)

Treatment with PFN, ionomycin, SLO and GzmB

Native human PFN and GzmB were purified from NK-YT cells and native rat PFN or GzmB from RNK16 cells as described.[18,19] Animal use was approved by the Animal Care and Use Committee of the Immune Disease Institute and Harvard Medical School. Ionomycin was from Sigma and purified SLO from BioAcademia Inc. (Osaka, Japan). Cells were washed and equilibrated 5 min in HBSS with 10 mM Hepes pH7.5, 4 mM $CaCl_2$, 0.4% BSA before adding PFN, ionomycin, SLO and/or GzmB, diluted in PFN buffer (HBSS, 10 mM Hepes pH7.5). Sublytic PFN, ionomycin and SLO concentrations were determined independently for each experiment as the concentration required to induce 5-15% propidium iodide (PI) uptake (2 μg/mL) (Sigma) measured 20 min later by flow cytometry (FACScalibur; Becton Dickinson).[18,19]

Immunostaining of EEA-1, GzmB and PFN

HeLa cells were grown on rat collagen-coated glass coverslips (Sigma) and treated with sublytic native human PFN (hPFN) and/or GzmB. After the indicated time, cells were fixed for 20 min in PBS/2% PFA, washed and incubated 20 min in PBS/50 mM NH_4Cl. Cells were then washed with PBS, permeabilized for 5 min in permeabilization buffer (PBS/0.2% Triton X-100). After 2 washes in PBS, coverslips were placed in blocking solution (PBS/10% FCS) for 30 min, washed once in PBS and incubated for 1 hr at RT with the indicated primary antibodies (mouse anti-human PFN, clone Pf80/164, Mabtech Inc.; goat anti-EEA-1, clone N19, SantaCruz Biotechnology Inc.; mouse anti-human GzmB, clone GB11, Caltag Laboratories) in incubation buffer (PBS/0.05% Triton X-100). Cells were then washed 3 times with incubation buffer and incubated 1 hr at RT with donkey Alexa-Fluor488 and/or 647-conjugated secondary antibodies (Molecular Probes) in incubation buffer containing 5% normal donkey serum (Sigma). Cells were then washed 3 times in PBS and mounted in Vectashield mounting medium containing DAPI (Vector Laboratories) before epifluorescence or spinning disk confocal imaging, as indicated (see supplemental methods).

Measurement of membrane-associated AP-2

Measurement of membrane-associated AP-2 puncta was performed as described previously.[20,21] All particle tracks were individually validated. Calculation of lifetime, maximal intensity distributions, and total number of puncta was performed using an image analysis application developed using Matlab 7 (Mathworks, Natick, MA).[21] The percent increase in AP-2-mediated endocytosis after treatment was calculated as: ((sum of maximum intensity of membrane-associated AP-2 spots after treatment/sum of maximum intensity of membrane-associated AP-2 spots before treatment)-1) x100.

Inhibition of endocytosis

siRNAs for GFP, μ2-adaptin (AP2μ2), clathrin heavy chain (CHC)[22], dynamin 2 (Dyn2) (ON-TARGETplus siRNA, Dharmacon) and flotillin-1 (Santa Cruz Biotechnology) were transfected into HeLa cells using Oligofectamine (100 nM final siRNA concentration, Invitrogen) according to the manufacturer's protocol. Cells were tested for knockdown 48 hr later by immunoblot probed with anti-AP-2 (clone AP50), anti-flotillin-1 (clone 18) (BD Transduction Laboratories), anti-CHC (clone X22, Affinity BioReagents) mouse monoclonal Abs, anti-Dyn2 (Calbiochem) or anti-α-tubulin (Affinity BioReagents) rabbit polyclonal Abs.

In some experiments, HeLa cells were pretreated 30 min before adding PFN and GzmB with 80 μM Dynasore, a cell permeable inhibitor of Dyn[23], in 0.8% DMSO or 300 mM sucrose (Sigma) in cell buffer without BSA. Potassium depletion was performed as described.[24]

Apoptosis and necrosis assays

To assess apoptosis, cells incubated for 2 hr at 37°C with buffer or sublytic rat PFN and/or 200 nM native human GzmB were analyzed for caspase activation by flow cytometry using M30-FITC mAb staining according to the manufacturer protocol (M30 CytoDEATH, Roche) to detect a caspase-cleavage product of cytokeratin 18 (CK18).[25] PFN-induced necrosis was assessed by flow cytometry 15 min after loading by PI staining (2 μg/mL in 10 mM Hepes pH 7.5, 140 mM NaCl, 2.5 mM $CaCl_2$ buffer).

Results

Perforin and granzymes are endocytosed into outsized early endosomes

To examine the effect of PFN on GzmB internalization, we incubated HeLa cells with native human GzmB (hGzmB) in the presence or absence of sublytic concentrations of native human PFN (hPFN). The sublytic concentration is the concentration that delivers Gzms to induce apoptosis without excessive necrosis.[11,18] As previously reported[11], hPFN greatly enhanced hGzmB uptake. Both hPFN and hGzmB were taken up within 5 min into large EEA-1+ intracellular vesicles which form after PFN treatment (**Figure 1A, B**). We termed these structures gigantosomes, since they are approximately an order of magnitude larger in diameter than other endosomes.[11] Because both anti human PFN and GzmB antibodies were from mouse, we were unable to costain hPFN and hGzmB in the same cells. However, staining with affinity-purified polyclonal antisera to purified rat NK cell GzmB and PFN, showed that PFN and GzmB colocalize in EEA-1+ vesicles when HeLa cells were loaded with sublytic native rat PFN and GzmB (**Figure S1A-D**). The enlargement of early endosomes was also selective, since when cells were analyzed 2 min after adding hPFN, EEA-1 vesicles increased in size, but Lamp-1 staining vesicles (a marker of late endosomes/lysosomes) remained approximately the same size (**Figure S2A**). Endocytosis of PFN was rapid (**Figure 1C**). 30 sec after adding sublytic hPFN to HeLa cells, PFN immunostaining was mostly at the plasma membrane and only few EEA-1+ endosomes stained for PFN. However, after 1 min, plasma membrane-associated PFN partitioned into EEA-1+ vesicles that evolved into gigantosomes within ~2-3 min.

Sublytic hPFN also greatly enhanced the uptake of fluorescent 70 kDa cationic dextran into large intracellular vesicles. Treatment of cells labeled with a fluorescent lipophilic dye (FM4-64) with sublytic rPFN or hPFN also induced rapid redistribution of the plasma membrane-associated dye to intracellular membranes (**Figure S2B).** However, uptake of transferrin (Tf), which binds to its receptor at the cell surface and is rapidly internalized by clathrin-mediated endocytosis in the absence of PFN, was not enhanced or accelerated by hPFN treatment (**Figures S2C, S2D**). However, Tf concentrated into gigantosomes, and Tf-containing gigantosomes co-stained with PFN (**Figure S2E**). Therefore, PFN activates rapid endocytosis of Gzms as well as other cell membrane-associated molecules into gigantosomes. Moreover, molecules which are normally rapidly endocytosed independently of PFN (such as Tf) localize into large endosomes when PFN is present. In the process, PFN is also removed from the plasma membrane to the gigantosome.

Cytotoxic T lymphocyte degranulation triggers gigantosome formation and PFN endocytosis in target cells

To determine whether PFN-containing gigantosomes also form in the physiologically relevant setting of CTL attack, we looked for gigantosome formation by live cell microscopy when HeLa cells expressing EGFP-EEA-1 were treated with HeLa cell-specific CTL. When cells were co-incubated with the Ca^{2+} chelator EGTA to allow effector/target conjugate formation but block cytotoxic granule exocytosis, the distribution of EGFP-EEA-1 was unchanged. However when Ca^{2+} was added to trigger CTL degranulation, large EEA-1+ vesicles were seen within a few minutes near the immunological synapse in the target cell, suggesting a localized effect of PFN (**Figure 2A, Movies S1, S2**). Gigantosomes were also generated in target cells when concanavalin A-coated HeLa cells were mixed with lymphokine-activated killer (LAK) cells (**Figure 2B**). Moreover, PFN co-localized with EEA-1 in the target cells. Therefore, PFN-containing EEA-1+ gigantosomes form in target cells attacked by human T cells.

Clathrin associates with gigantosomes

Our next goal was to define the endocytic pathway triggered by PFN. Endocytosis can be mediated by both clathrin-dependent and clathrin-independent pathways, including endocytosis via caveolin or flotillin vesicles, phagocytosis, macropinocytosis and trans-endocytosis.[26] Since clathrin-mediated endocytosis is a major endocytic pathway, we used

both fixed and live cell imaging to examine whether PFN-induced gigantosomes associate with clathrin. Gigantosomes formed after sublytic rPFN treatment stain for EEA-1 and Clathrin Heavy Chain (CHC), but do not stain for caveolin-1, flotillin-1 (involved in clathrin-independent endocytosis) or Lamp-1 (CD107a) (**Figure S3A**). To examine gigantosome formation without potential fixation artifacts, HeLa cells, stably expressing EGFP-Clathrin Light Chain (CLC) and transiently transfected with mRFP-EEA-1, were treated with sublytic rPFN and imaged by live cell confocal microscopy (**Figures 3, S3B**). After adding PFN, early endosomes rapidly enlarged to form vesicles that partially immunostained with clathrin. Indeed, 3D capture images showed that clathrin partially coated the gigantosomes (**Movies S3, S4**). The accumulation of clathrin in gigantosomes suggests that clathrin might be involved in gigantosome formation.

PFN treatment enhances clathrin-coated pit formation and clathrin-mediated endocytosis

Since gigantosomes associate with clathrin, we wanted to know whether PFN or two other agents known to trigger cellular "wound-healing", ionomycin[11] and SLO[17], might enhance clathrin-mediated endocytosis. As previously described, sublytic concentrations of rPFN, SLO and ionomycin activate wound healing, without necrosis, as confirmed by detecting externalization of the lumenal lysosomal marker Lamp-1, but not PI uptake (**Figures S4A-C**).[11,27] Gigantosomes also formed after sublytic ionomycin or SLO treatment (**Figure S4D**), suggesting that gigantosome formation may be a general feature of the response to increased intracellular Ca^{2+}, which activates both homotypic and heterotypic fusion of membrane-delimited vesicles.[11,17] Both sublytic rPFN and SLO enhanced uptake of GzmB labeled with Alexa488 (A488-GzmB), but even the highest concentration of ionomycin did not (as previously reported[11]) (**Figure 4A**). To determine whether rPFN and SLO-mediated enhanced uptake of GzmB might be secondary to enhanced clathrin-mediated endocytosis, we analyzed the effect of these three membrane-perturbing agents on the rate of clathrin-dependent endocytosis using spinning disc confocal microscopy. The number, maximum fluorescence intensity (proportional to the size of coated-vesicles) and lifetime of new clathrin-coated pits (CCP) forming at the plasma membrane, identified as AP-2 clathrin adaptor spots[20,21], were quantified before and after adding sublytic rPFN, SLO or ionomycin to HeLa cells stably expressing an EGFP-tagged σ2 subunit of the clathrin adaptor AP-2 complex (EGFP-AP2σ2) (**Figures 4B-E; Movies S5-S7**). Sublytic rPFN and SLO significantly increased both the number of new plasma-membrane associated AP-2 puncta and their total intensity, while ionomycin (5 μM) did not. Moreover, a slightly higher, but still sublytic, concentration (7

μM) of ionomycin led to a rapid and dramatic loss of all membrane-associated AP-2 within ~2 min (**Figure S4E**), suggesting disruption of CCP formation. In addition, the majority of AP-2 spots newly-formed in the presence of rPFN and SLO disappeared quickly from the visual field (lifetime ≈ 50-200 sec), suggesting clathrin-coated vesicles (CCV) formed normally after treatment with PFN or SLO and were transported deeper in the cytosol. The percent increase in AP-2/clathrin-mediated endocytosis was calculated from the change in the total fluorescence intensity of new membrane-associated AP-2 puncta formed in the same cell before and after treatment. Sublytic rPFN and SLO significantly increased AP-2-mediated endocytosis by ~110±38% and 65±7%, respectively, but the slight increase with ionomycin (~14±13%) was not significant (**Figure 4E**). To understand the reason for the differing effects of PFN, SLO and ionomycin on clathrin-mediated endocytosis, we measured the Ca^{2+} flux induced by these three agents. Sublytic concentrations of all three led to increased intracellular Ca^{2+} (**Figure 4F**). However, the increase in intracellular Ca^{2+} was transient in cells treated with sublytic rPFN or SLO, but sustained and greater after 5 μM ionomycin. Similar data were obtained after treatment with 1-10 μM ionomycin (not shown). Therefore, a transient cytosolic Ca^{2+} rise seems to be required to trigger enhanced endocytosis, while a sustained increase in intracellular Ca^{2+}, as produced by ionomycin, may disrupt clathrin-mediated endocytosis, as has been reported.[28]

Inhibiting dynamin and clathrin-mediated endocytosis increases PFN-induced necrosis

Because endocytosis removes PFN from the plasma membrane, we hypothesized that inhibiting endocytosis might increase necrotic cell death caused by persistence of PFN pores in the plasma membrane. Moreover, since PFN increases AP2-mediated endocytosis, we hypothesized that PFN is removed from the plasma membrane by a clathrin-dependent mechanism that also relies on Dyn2, a ubiquitously expressed GTPase that plays an essential role in vesicle scission during both clathrin-mediated and clathrin-independent endocytosis.[29] (The other Dyn isoform (Dyn1) is not expressed in HeLa cells.) To investigate whether inhibiting endocytosis enhances PFN-induced necrosis, PI uptake was measured 15 min after adding PFN to HeLa cells pretreated with inhibitors of Dyn and clathrin-dependent endocytosis. Pretreatment with hypertonic sucrose, potassium depletion (which interfere with the clathrin pathway by dispersing clathrin lattices on the plasma membrane[30]) or Dynasore (a small molecule Dyn2 inhibitor[23]) increased necrosis induced by sublytic and lytic rPFN concentrations (**Figures S5A, S5B**). Similarly, hypertonic sucrose and Dynasore increased

necrosis by SLO (**Figures S5C, S5D**). However, because some of these inhibitors are not specific[31], we confirmed our data by knocking down key genes involved in Dyn/clathrin-dependent endocytosis by transfecting siRNAs to clathrin heavy chain (CHC), the μ2 subunit of AP-2 adaptor (AP-2μ2)[22] or Dyn2 (**Figure S5E**). EGFP siRNAs were used as an irrelevant control and flotillin-1 siRNAs as a negative control for clathrin-independent endocytosis. As expected, Tf uptake was decreased in cells knocked down for CHC, AP2-μ2 or Dyn2, but not in cells treated with flotillin-1 or GFP siRNAs (not shown). HeLa cells transfected with Dyn2, AP2μ2 and CHC siRNAs were more prone to necrosis induced by sublytic or lytic rPFN than cells transfected with flotillin-1 or control siRNAs (**Figures 5A-C**). These experiments confirm that Dyn/clathrin-dependent endocytosis preserves membrane integrity, likely by removing PFN (and SLO) pores from the plasma membrane.

Inhibiting dynamin and clathrin decreases PFN-induced GzmB uptake

Because PFN and GzmB are endocytosed into the same EEA-1+ compartment, we hypothesized that GzmB internalization is also clathrin- and Dyn2-dependent. Previous studies have come to contradictory conclusions about whether PFN-mediated endocytosis of GzmB is Dyn2-dependent.[32,33] To investigate whether GzmB uptake is Dyn/clathrin-dependent, we again used chemical and siRNAs to inhibit Dyn/clathrin endocytosis. Pretreatment with hypertonic sucrose or Dynasore strongly decreased A448-GzmB internalization after sublytic rPFN treatment (**Figure 6A, 6B**). Similarly transfection of CHC, AP-2μ2 and Dyn2, but not flotillin-1 or control, siRNAs inhibited rPFN-facilitated A488-GzmB uptake as assessed by either flow cytometry or fluorescence microscopy (**Figures 6C, 6D**). Therefore, PFN-induced uptake of GzmB requires Dyn2 and clathrin. Moreover, since inhibiting PFN-activated endocytosis increases PFN-induced necrosis probably by increasing the number of PFN pores persisting at the cell surface, but decreases GzmB uptake, it is unlikely that GzmB enters the cell by plasma membrane PFN pores.

Inhibiting dynamin- and clathrin-mediated endocytosis decreases PFN and GzmB-induced apoptosis

We previously showed that when the plasma membrane "wound-healing" response is inhibited by chelating intracellular Ca^{2+}, cells treated with PFN and GzmB are more likely to die by necrosis than by apoptosis.[11] We suspected that a similar shift in the balance between apoptosis and necrosis would occur when endocytosis is inhibited. To test this idea, we compared caspase activation by measuring CK18 cleavage in HeLa cells pretreated or not

with hypertonic sucrose or Dynasore. Cells treated with these inhibitors were significantly less likely to die by apoptosis after rPFN and hGzmB treatment (**Figures 7A, 7B**). Similarly, HeLa cells transfected with Dyn2, AP2-μ2 or CHC siRNAs were significantly less likely to undergo apoptosis than cells transfected with control or flotillin-1 siRNAs, when apoptosis was measured either by caspase activation (**Figures 7C-D**) or by counting apoptotic nuclei after DAPI staining (**Figures S6A**). Because SLO has been extensively used to substitute for PFN to deliver GzmB to target cells, we also tested whether inhibition of Dyn and clathrin-mediated endocytosis impairs apoptosis by SLO/GzmB. Although a previous report suggested that SLO-induced endocytosis of dextran is Dyn-independent[17], we found that SLO and GzmB-mediated apoptosis in HeLa cells was significantly decreased by hypertonic sucrose or Dynasore treatment (**Figures S6B, S6C**), suggesting that apoptosis caused by GzmB and PFN (or SLO) is indeed Dyn2 and clathrin-dependent. When endocytosis was inhibited, PFN-mediated necrosis increased, while PFN delivery of GzmB to induce apoptosis was inhibited. To confirm these data, we next measured CTL-induced cell death by ^{51}Cr release assay, which doesn't distinguish between apoptosis and necrosis, in HeLa cells transfected with Dyn2, AP2-μ2, or CHC siRNAs. The overall amount of cell death in Dyn2, AP2-μ2, or CHC siRNA-treated cells was comparable to that of control cells (**Figure 7E**). Therefore clathrin and Dyn-dependent endocytosis does not affect whether a cell dies, but influences how it dies. Taken together, these experiments strongly suggest that PFN-mediated GzmB delivery into target cells is Dyn2 and clathrin-dependent and that endocytosis of PFN helps maintain membrane integrity to protect cells from necrosis and allow them to undergo the slower process of apoptosis.[16]

Discussion

PFN creates pores in the target cell plasma membrane, transiently allowing Ca^{2+} into the cell. The Ca^{2+} influx triggers a wounded-membrane repair response, where lysosomes and endosomes fuse to the plasma membrane to reseal the damaged membrane. The wound-healing response protects target cells from necrosis and allows them to undergo the slower, ATP-dependent process of Gzm-mediated apoptosis[11]. We now show that PFN also triggers the rapid clathrin and Dyn-dependent endocytosis of GzmB and PFN into enlarged EEA-1+ early endosomes, we term gigantosomes. Rapid and enhanced endocytosis serves two important functions (1) to remove the membrane-damaging agent (PFN) from the membrane and (2) to internalize PFN and Gzms - the critical first step of PFN-mediated intracellular

delivery of Gzms to initiate target cell apoptosis. For the first time we have been able to detect PFN within target cells, both in cells treated with native PFN or subjected to CTL attack. PFN concentrates with GzmB into gigantosomes. Therefore we postulate a two-step model for PFN – first multimerization at the plasma membrane to create small pores that trigger a wound healing response that increases endocytosis of Gzms and PFN into gigantosomes and then disruption of the gigantosome membrane to release Gzms to the cytosol. Understanding the latter step is outside the scope of this study, but our model is that PFN multimerizes in the gigantosome membrane to form larger pores that release Gzms into the cytosol. Indeed we see Gzms in the cytosol within ~15-20 min of adding Gzms and PFN and then Gzms concentrate in the nucleus and mitochondria (Fig. 6D, data not shown). Although some results were demonstrated with rat and some with human PFN, we have found these sources of PFN to function indistinguishably in these assays. Moreover many of these experiments were also performed by substituting GzmA for GzmB, with comparable results (not shown). Therefore, we expect our findings apply to PFN delivery of all Gzms.

Internalization of Gzms does not require a cell-specific receptor[32,34,35], although binding to mannose receptors may enhance uptake[36-38]. This means that PFN-mediated delivery can deliver Gzms to all cells, irrespective of their cell surface protein expression. Indeed, binding and uptake of GzmB via PFN is not blocked by trypsinizing cells, but is blocked by interfering with ionic interactions.[37,39] PFN indiscriminately induces capture into gigantosomes of other cationic molecules, such as cationic dextrans, bound to the plasma membrane in a receptor-independent manner by charge, as well as receptor-bound molecules, like Tf. Although many of our results were obtained by loading PFN and GzmB into target cells, we also verified their relevance by visualizing gigantosome formation and PFN co-localization in gigantosomes in target cells within minutes of CTL attack. It should be mentioned that GzmB can be endocytosed inefficiently and slowly in the absence of PFN.[13,40] However unless co-endocytosed with PFN, GzmB is unable to escape from endosomes to activate apoptosis.[39] By a combination of knockdown and inhibitor experiments, we showed that PFN delivery of GzmB is clathrin and Dyn dependent. In fact, PFN treatment increases the recruitment of the AP-2 adaptor complex to the plasma membrane, which is essential for clathrin-mediated endocytosis.

When endocytosis is inhibited in target cells treated with GzmB and PFN, the balance between necrotic and apoptotic cell death shifts, PFN-mediated necrosis increases, while

delivery of GzmB to induce apoptosis is inhibited. Therefore, the endocytic component of the plasma membrane repair response, which removes PFN from the plasma membrane, is required to direct immune-mediated cell death by CTLs and NK cells towards apoptosis and to prevent the inflammation that occurs in response to necrotic cells.[16] This finding of a Dyn-dependent alteration in the balance between necrotic and apoptotic death explains the seemingly contradictory results of other groups. Trapani and colleagues concluded that PFN delivery of Gzms is Dyn-independent based only on cell survival assays, which measure both apoptosis and necrosis[32], while Bleackley's group found that GzmB and PFN-induced apoptosis, measured by caspase activation, is Dyn-dependent.[33] Our findings that overall cell death is not altered by inhibiting Dyn2, but that apoptosis induction requires Dyn2 are consistent with both studies and explain how these seemingly inconsistent results can both hold.

Rapid endocytosis to remove membrane-damaging agents may be a general feature of the plasma-membrane repair response, since it is also seen with SLO, as previously reported[17] and confirmed here. We also confirmed that SLO enhances clathrin-mediated endocytosis, as previously reported.[17] However, unlike the previous report, we found that SLO-triggered endocytosis is also Dyn-dependent, based on experiments using a Dyn inhibitor and siRNAs. The Idone et al. study[17] based their conclusion that SLO-mediated endocytosis is Dyn-independent on experiments using cells expressing K44A Dyn2 and cholesterol extraction with methyl-β-cyclodextrin (MβCD) to conclude that SLO-mediated internalization depends on endocytic pathways specific for cholesterol-rich membrane domains. However, MβCD treatment can also perturb formation of CCV.[31] Moreover, Dyn is also used for vesicle scission in clathrin-independent pathways.

Although PFN and SLO both activate the damaged plasma membrane repair response[11,41], increase clathrin-mediated endocytosis and induce GzmB uptake into endosomes, ionomycin, a Ca^{2+} ionophore which triggers the first feature of cellular wound-healing (fusion of lysosomes with the plasma membrane), does not induce GzmB endocytosis. A salient difference between ionomycin and SLO or PFN is that the rise in intracellular Ca^{2+} by ionomycin is higher and persists, while for SLO and PFN it is transient. A recent study showed that the plasma membrane repair response to SLO only operates when intracellular Ca^{2+} is in the range of 5-10 μM[42], suggesting that high intracellular Ca^{2+} after ionomycin

treatment may prevent plasma membrane repair, especially endocytosis. Ionomycin also differs from the other agents by its mechanism of action. The Ca^{2+} flux induced by ionomycin originates from both mobilization of intracellular stores and an influx of extracellular Ca^{2+}.[43] Since ionomycin depletes Ca^{2+} from mitochondria, disrupts the mitochondrial transmembrane potential and ATP generation, it may deplete the cell of the energy needed for endocytosis.[44] Ionomycin is known to lead to a dramatic loss of clathrin puncta and dissociation of endocytic adaptors from the plasma membrane.[28] In fact, sublytic concentrations of ionomycin actually inhibit clathrin-mediated endocytosis.[45]

In our previous study when we blocked vesicular exocytosis in the membrane repair response by chelating intracellular Ca^{2+}, we also blocked the endocytic part of the response.[11] Here, we selectively blocked endocytosis using chemical inhibitors and siRNAs directed against key endocytic molecules and showed that endocytosis activated during membrane repair is critical for avoiding necrosis and permitting PFN to deliver GzmB to activate apoptotic death. Finding a way to block vesicular exocytosis selectively would enable researchers to evaluate whether endocytosis is activated to remove the extra plasma membrane added during vesicular membrane fusion and to assess the relative contributions of these two repair processes in preventing necrosis during immune cell-mediated death. Because CTL degranulation and PFN membrane binding and multimerization are all Ca^{2+}-dependent processes, the simplest maneuvers of chelating Ca^{2+}, either within cells or in the extracellular fluid, have multiple effects on PFN function. Therefore, dissecting the contributions of different components of membrane repair caused by pore-forming proteins may be more straightforward by studying Ca^{2+}-independent pore-forming proteins, like SLO, than PFN.

Acknowledgments

We thank Eric Marino for assistance with microscopy and Sonia Sharma for experimental assistance. This work was supported by NIH AI063430 (JL) and fellowships from the Swiss National Science Foundation (MW) and the Human Frontier Science Program Organization (EB).

Authorship

Contribution: J.T. designed and performed experiments, analyzed data and wrote the manuscript. D.K., S.S., D.M., M.W. and E.B. also performed and helped analyze some

experiments. T.K. and J.L. conceived and supervised the project, helped design experiments and coordinated the writing of the manuscript.

Conflict of interest disclosure: The authors declare no competing financial interests.

References

1. Stinchcombe JC, Bossi G, Booth S, Griffiths GM. The immunological synapse of CTL contains a secretory domain and membrane bridges. *Immunity*. 2001;15(5):751-761.

2. Chowdhury D, Lieberman J. Death by a thousand cuts: granzyme pathways of programmed cell death. *Annu Rev Immunol*. 2008;26:389-420.

3. Masson D, Tschopp J. Isolation of a lytic, pore-forming protein (perforin) from cytolytic T-lymphocytes. *J Biol Chem*. 1985;260(16):9069-9072.

4. Podack ER, Young JD, Cohn ZA. Isolation and biochemical and functional characterization of perforin 1 from cytolytic T-cell granules. *Proc Natl Acad Sci U S A*. 1985;82(24):8629-8633.

5. Kagi D, Ledermann B, Burki K, et al. Cytotoxicity mediated by T cells and natural killer cells is greatly impaired in perforin-deficient mice. *Nature*. 1994;369(6475):31-37.

6. Stepp SE, Dufourcq-Lagelouse R, Le Deist F, et al. Perforin gene defects in familial hemophagocytic lymphohistiocytosis. *Science*. 1999;286(5446):1957-1959.

7. Pipkin ME, Lieberman J. Delivering the kiss of death: progress on understanding how perforin works. *Curr Opin Immunol*. 2007;19(3):301-308.

8. Voskoboinik I, Smyth MJ, Trapani JA. Perforin-mediated target-cell death and immune homeostasis. *Nat Rev Immunol*. 2006;6(12):940-952.

9. Millard PJ, Henkart MP, Reynolds CW, Henkart PA. Purification and properties of cytoplasmic granules from cytotoxic rat LGL tumors. *J Immunol*. 1984;132(6):3197-3204.

10. Tschopp J, Masson D, Stanley KK. Structural/functional similarity between proteins involved in complement- and cytotoxic T-lymphocyte-mediated cytolysis. *Nature*. 1986;322(6082):831-834.

11. Keefe D, Shi L, Feske S, et al. Perforin triggers a plasma membrane-repair response that facilitates CTL induction of apoptosis. *Immunity*. 2005;23(3):249-262.

12. Metkar SS, Wang B, Aguilar-Santelises M, et al. Cytotoxic cell granule-mediated apoptosis: perforin delivers granzyme B-serglycin complexes into target cells without plasma membrane pore formation. *Immunity*. 2002;16(3):417-428.

13. Froelich CJ, Orth K, Turbov J, et al. New paradigm for lymphocyte granule-mediated cytotoxicity. Target cells bind and internalize granzyme B, but an endosomolytic agent is necessary for cytosolic delivery and subsequent apoptosis. *J Biol Chem.* 1996;271(46):29073-29079.

14. Reddy A, Caler EV, Andrews NW. Plasma membrane repair is mediated by Ca(2+)-regulated exocytosis of lysosomes. *Cell*. 2001;106(2):157-169.

15. McNeil PL, Kirchhausen T. An emergency response team for membrane repair. *Nat Rev Mol Cell Biol*. 2005;6(6):499-505.

16. Savill J, Fadok V. Corpse clearance defines the meaning of cell death. *Nature*. 2000;407(6805):784-788.

17. Idone V, Tam C, Goss JW, et al. Repair of injured plasma membrane by rapid Ca2+-dependent endocytosis. *J Cell Biol*. 2008;180(5):905-914.

18. Martinvalet D, Thiery J, Chowdhury D. Chapter eleven granzymes and cell death. *Methods Enzymol*. 2008;442:213-230.

19. Thiery J, Walch M, Jensen DK, Martinvalet D, Lieberman J. Isolation of cytotoxic T cell and NK granules and purification of their effector proteins. *Current Protocols in Cell Biology*. in press

20. Ehrlich M, Boll W, Van Oijen A, et al. Endocytosis by random initiation and stabilization of clathrin-coated pits. *Cell*. 2004;118(5):591-605.

21. Saffarian S, Kirchhausen T. Differential evanescence nanometry: live-cell fluorescence measurements with 10-nm axial resolution on the plasma membrane. *Biophys J*. 2008;94(6):2333-2342.

22. Motley A, Bright NA, Seaman MN, Robinson MS. Clathrin-mediated endocytosis in AP-2-depleted cells. *J Cell Biol*. 2003;162(5):909-918.

23. Macia E, Ehrlich M, Massol R, et al. Dynasore, a cell-permeable inhibitor of dynamin. *Dev Cell*. 2006;10(6):839-850.

24. Madshus IH, Sandvig K, Olsnes S, van Deurs B. Effect of reduced endocytosis induced by hypotonic shock and potassium depletion on the infection of Hep 2 cells by picornaviruses. *J Cell Physiol*. 1987;131(1):14-22.

25. Leers MP, Kolgen W, Bjorklund V, et al. Immunocytochemical detection and mapping of a cytokeratin 18 neo-epitope exposed during early apoptosis. *J Pathol*. 1999;187(5):567-572.

26. Doherty GJ, McMahon HT. Mechanisms of Endocytosis. *Annu Rev Biochem*. 2009;78:857-902.

27. Rodriguez A, Webster P, Ortego J, Andrews NW. Lysosomes behave as Ca2+-regulated exocytic vesicles in fibroblasts and epithelial cells. *J Cell Biol*. 1997;137(1):93-104.

28. Zoncu R, Perera RM, Sebastian R, et al. Loss of endocytic clathrin-coated pits upon acute depletion of phosphatidylinositol 4,5-bisphosphate. *Proc Natl Acad Sci U S A*. 2007;104(10):3793-3798.

29. Hinshaw JE. Dynamin and its role in membrane fission. *Annu Rev Cell Dev Biol*. 2000;16:483-519.

30. Hansen SH, Sandvig K, van Deurs B. Molecules internalized by clathrin-independent endocytosis are delivered to endosomes containing transferrin receptors. *J Cell Biol*. 1993;123(1):89-97.

31. Ivanov AI. Pharmacological inhibition of endocytic pathways: is it specific enough to be useful? *Methods Mol Biol*. 2008;440:15-33.

32. Trapani JA, Sutton VR, Thia KY, et al. A clathrin/dynamin- and mannose-6-phosphate receptor-independent pathway for granzyme B-induced cell death. *J Cell Biol*. 2003;160(2):223-233.

33. Veugelers K, Motyka B, Frantz C, et al. The granzyme B-serglycin complex from cytotoxic granules requires dynamin for endocytosis. *Blood*. 2004;103(10):3845-3853.

34. Dressel R, Raja SM, Honing S, et al. Granzyme-mediated cytotoxicity does not involve the mannose 6-phosphate receptors on target cells. *J Biol Chem*. 2004;279(19):20200-20210.

35. Kurschus FC, Bruno R, Fellows E, Falk CS, Jenne DE. Membrane receptors are not required to deliver granzyme B during killer cell attack. *Blood*. 2005;105(5):2049-2058.

36. Motyka B, Korbutt G, Pinkoski MJ, et al. Mannose 6-phosphate/insulin-like growth factor II receptor is a death receptor for granzyme B during cytotoxic T cell-induced apoptosis. *Cell*. 2000;103(3):491-500.

37. Bird CH, Sun J, Ung K, et al. Cationic sites on granzyme B contribute to cytotoxicity by promoting its uptake into target cells. *Mol Cell Biol*. 2005;25(17):7854-7867.

38. Veugelers K, Motyka B, Goping IS, et al. Granule-mediated killing by granzyme B and perforin requires a mannose 6-phosphate receptor and is augmented by cell surface heparan sulfate. *Mol Biol Cell*. 2006;17(2):623-633.

39. Shi L, Keefe D, Durand E, et al. Granzyme B binds to target cells mostly by charge and must be added at the same time as perforin to trigger apoptosis. *J Immunol*. 2005;174(9):5456-5461.

40. Pinkoski MJ, Hobman M, Heibein JA, et al. Entry and trafficking of granzyme B in target cells during granzyme B-perforin-mediated apoptosis. *Blood*. 1998;92(3):1044-1054.

41. McNeil PL, Steinhardt RA. Plasma membrane disruption: repair, prevention, adaptation. *Annu Rev Cell Dev Biol*. 2003;19:697-731.

42. Babiychuk EB, Monastyrskaya K, Potez S, Draeger A. Intracellular Ca(2+) operates a switch between repair and lysis of streptolysin O-perforated cells. *Cell Death Differ*. 2009;16(8):1126-1134.

43. Dedkova EN, Sigova AA, Zinchenko VP. Mechanism of action of calcium ionophores on intact cells: ionophore-resistant cells. *Membr Cell Biol*. 2000;13(3):357-368.

44. Gmitter D, Brostrom CO, Brostrom MA. Translational suppression by Ca2+ ionophores: reversibility and roles of Ca2+ mobilization, Ca2+ influx, and nucleotide depletion. *Cell Biol Toxicol*. 1996;12(2):101-113.

45. Cousin MA, Robinson PJ. Ca(2+) influx inhibits dynamin and arrests synaptic vesicle endocytosis at the active zone. *J Neurosci*. 2000;20(3):949-957.

Figure Legends

Figure 1. PFN and GzmB are rapidly endocytosed into EEA-1+ outsized early endosomes.

(A-B) Within 5 min of treatment with sublytic native hPFN and hGzmB, large intracellular and membrane bound endosomes (gigantosomes) co-immunostain for GzmB (A) or PFN (B) and the early endosomal marker EEA-1. Images were acquired by widefield fluorescence microscopy and deconvolved using iterative deconvolution. Representative Z stack series projections from three independent experiments are shown. Percentage of cells with GzmB or PFN-staining enlarged endosomes is indicated (mean ± s.d.). **(C)** HeLa cells were exposed to sublytic hPFN for indicated times and stained for PFN and EEA-1. PFN is first detected at the plasma membrane and then gradually endocytosed into EEA-1+ endosomes before forming gigantosomes. Representative confocal sections from three independent experiments are shown. PFN or GzmB was detected using AlexaFluor 488-conjugated secondary antibody and EEA-1 using AlexaFluor 647-conjugated secondary antibody. Color bars and associated numbers indicate fluorescence intensity levels. Scale bars, 10 μm. Dashed lines, plasma membrane.

Figure 2. Large endosomes ("gigantosomes") form in target cells within minutes of triggering CTL degranulation.

(A) Large EEA-1+ endosomes form in a target cell after CTL degranulation. EGFP-EEA-1 transfected HeLa target cells were incubated with specific CTL in the presence of EGTA to allow conjugate formation. After 2 min, $CaCl_2$ was added to induce CTL degranulation (bottom) (**images from movies S1 and S2**). Enlarged endosomes form in the target cell within min following CTL degranulation, while the size of early endosomes does not change in the absence of calcium (top). Data (deconvolved widefield images) are representative of three independent experiments. **(B)** Large endosomes formed in target cells after CTL attack contain PFN. ConA-coated HeLa cells were incubated with LAK cells in the presence of

EGTA to allow conjugate formation and then buffer (top) or $CaCl_2$ (bottom) was added to induce cytotoxic granule exocytosis 5 min before fixation. Data depicted (deconvolved widefield 3D images followed by Z-projection) are representative of two independent experiments. PFN signal was detected using AlexaFluor 488-conjugated secondary antibody and EEA-1 using AlexaFluor 647-conjugated secondary antibody. Color bars and associated numbers indicate fluorescence intensity levels. Scale bars, 10 μm. Dashed lines, plasma membrane.

Figure 3. Gigantosomes are coated with clathrin.

HeLa cells stably expressing EGFP-CLC (green) and transfected with mRFP-EEA-1 (red) were analyzed by live three-dimensional confocal capture 10 min following sublytic rPFN treatment. In the presence of rPFN, gigantosomes stained with EEA-1 (red), co-localize with clathrin (green) as indicated. One representative optical section obtained from sequential 0.1 μm optical sections (see **movies S3 and S4)** is shown for each condition. Most of the gigantosomes (red) are coated with clathrin (green). Data are representative of five independent experiments. Color bars and associated numbers indicate fluorescence intensity levels. Scale bars, 10 μm. Dashed lines, plasma membrane.

Figure 4. Perforin increases clathrin-mediated endocytosis

(A) Within 7 min of treatment, sublytic rPFN and SLO activate uptake of A488-GzmB, while ionomycin, even at the highest lytic concentration, does not. Mean fluorescence intensity (mean ± s.d.) from three independent experiments is indicated. **(B)** rPFN and SLO increase the rate of AP-2-dependent endocytosis, but ionomycin does not. HeLa cells stably expressing EGFP-AP-2σ2 were used for spatial and temporal analysis of AP-2 at CCPs. Cells were imaged every 10 sec by spinning disk confocal microscopy before and after addition of sublytic rPFN, ionomycin or SLO. The maximum fluorescence intensity and lifetime of new membrane-associated AP2 spots were measured 400 sec before and after treatment. Representative data from one cell treated with rPFN, ionomycin or SLO **(**Movies 3, 4 and 5**)** are shown. **(C-D)** Sublytic rPFN and SLO significantly increase the number of new AP2 spots associated with the plasma membrane and the total intensity of membrane-associated AP-2 molecules, while ionomycin (5 μM) only slightly increases membrane-associated AP-2. Data depicted were obtained from 3 different cells and 3 independent experiments. Data depicted in (B) correspond to cell #3 for each treatment. **(E)** The percentage increase of AP-2-mediated

endocytosis after treatment (mean ± s.d.) was calculated. **(F)** Intracellular Ca^{2+} increases following sublytic rPFN, SLO and ionomycin treatment. Calcium influx was measured by FlexStation III in HeLa cells stained with Fura-2/AM at 5 sec intervals after adding PFN, SLO or ionomycin. At sublytic concentrations, rPFN and SLO induce a transient Ca^{2+} flux, while ionomycin induces a sustained and global rise of intracellular Ca^{2+}. Data are representative of three independent experiments.

Figure 5. Inhibiting clathrin-mediated endocytosis increases PFN-induced necrosis

Inhibition of Dyn/clathrin-dependent endocytosis increases necrotic cell death following sublytic rPFN treatment. HeLa cells were transfected with siRNAs for Dyn2, AP2μ2, and CHC or pretreated with Dynasore (80 μM), an inhibitor of Dyn GTPase function, and then incubated for 15 min with sublytic rPFN. GFP (ctrl) or Flotillin-1 siRNAs were used as negative controls. Necrosis was evaluated immediately by flow cytometry measurement of PI uptake. Representative histograms after sublytic rPFN treatment **(A)**, and mean ± s.d. from three independent experiments with sublytic **(B)** or different doses of rPFN **(C)** are shown. (*, $p<0.03$, #, $p<0.001$, relative to control siRNA-treated cells).

Figure 6. Clathrin-mediated endocytosis is required for PFN-mediated GzmB internalization

(A-B) Inhibition of Dyn/clathrin-mediated endocytosis by pretreatment with hypertonic sucrose (300 mM) or Dynasore (80 μM) decreases sublytic rPFN-induced A488-GzmB internalization. **(C)** Cells transfected with Dyn2, AP-2μ2 or CHC siRNAs show reduced GzmB internalization, compared to control cells treated with GFP (ctrl) or Flotillin-1 siRNAs, 5 min after incubation with sublytic rPFN and A488-GzmB. Graphs are representative of three independent experiments and mean fluorescence intensity (MFI) (mean ± s.d.) are indicated. **(D)** Concentration of A488-GzmB (green) in the nucleus of target cells 20 min after sublytic rPFN and A488-GzmB incubation is seen in cells treated with flotillin-1 or GFP (Ctrl) siRNAs but not in cells treated with CHC siRNA. Numbers indicate the percentage of cells with nuclear GzmB (mean ± s.d. from three independent experiments). GzmB signal was detected using AlexaFluor 488-conjugated secondary antibody and EEA-1 using AlexaFluor 647-conjugated secondary antibody. Color bars and associated numbers indicate fluorescence intensity levels. Dashed lines, nuclei. Scale bar, 10 μm**.**

Figure 7. Inhibition of clathrin-mediated endocytosis reduces PFN and GzmB-mediated apoptosis, but does not alter the extent of CTL-mediated death

(A-B) Chemical inhibitors of clathrin-mediated endocytosis decrease PFN and GzmB-induced apoptosis. HeLa cells were preincubated with or without hypertonic sucrose or Dynasore before treatment with buffer or sublytic rPFN and/or GzmB. Apoptosis was measured 2 hr later by caspase activation by labeling with M30 mAb. Representative flow cytometry histogram **(A)** or mean ± s.d. from three independent experiments **(B)** are depicted. (**, $p<0.005$ relative to control siRNA-treated cells). **(C-D)** Specific inhibition of Dyn/clathrin-mediated endocytosis with siRNAs decreases PFN and GzmB-induced apoptosis. HeLa cells were transfected with indicated siRNAs before treatment with rPFN and/or GzmB and apoptosis was measured as in (**A,B**). Representative flow cytometry histogram **(C)** and mean ± s.d. from three independent experiments **(D)** are shown (**, $p<0.005$ relative to control siRNA-transfected cells). **(E)** Inhibition of Dyn/clathrin-mediated endocytosis does not interfere with overall CTL-induced cell death evaluated by ^{51}Cr release assay. HeLa cells transfected with indicated siRNAs were incubated for 4 hr with specific CTL. The data (mean ± s.d.) were obtained from two independent experiments performed in triplicate.

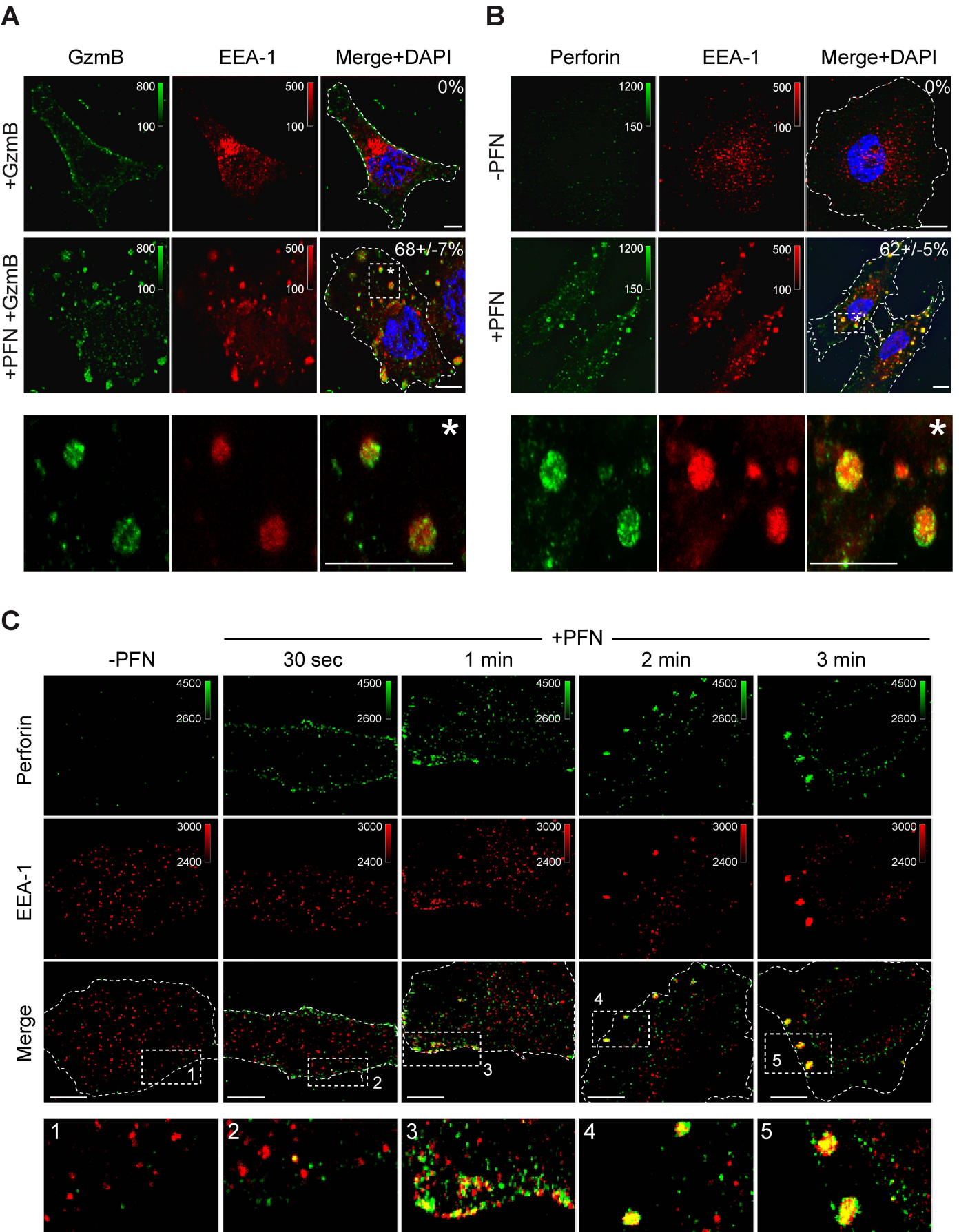
A
GzmB
EEA-1
Merge+DAPI
+GzmB
+PFN +GzmB
800
100
500
100
0%
68+/-7%
B
Perforin
EEA-1
Merge+DAPI
-PFN
+PFN
1200
150
500
100
0%
62+/-5%
C
-PFN
+PFN
30 sec
1 min
2 min
3 min
Perforin
EEA-1
Merge
4500
2600
3000
2400
1
2
3
4
5

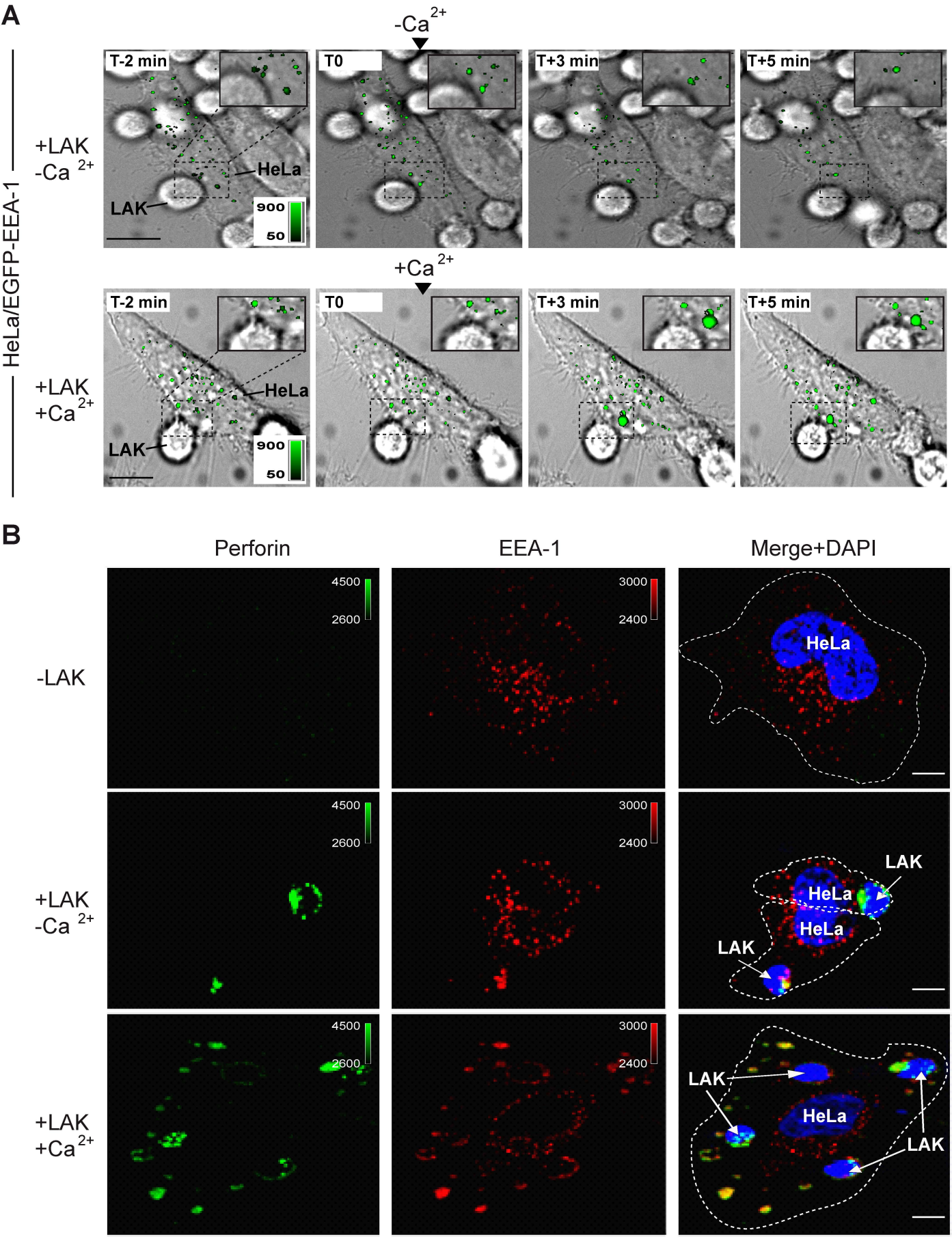
A
-Ca 2+
T-2 min
T0
T+3 min
T+5 min
+LAK
-Ca 2+
HeLa
LAK
900
50
+Ca 2+
+LAK
+Ca 2+
HeLa/EGFP-EEA-1
B
Perforin
EEA-1
Merge+DAPI
-LAK
+LAK
-Ca 2+
+LAK
+Ca 2+
4500
2600
3000
2400
HeLa
LAK

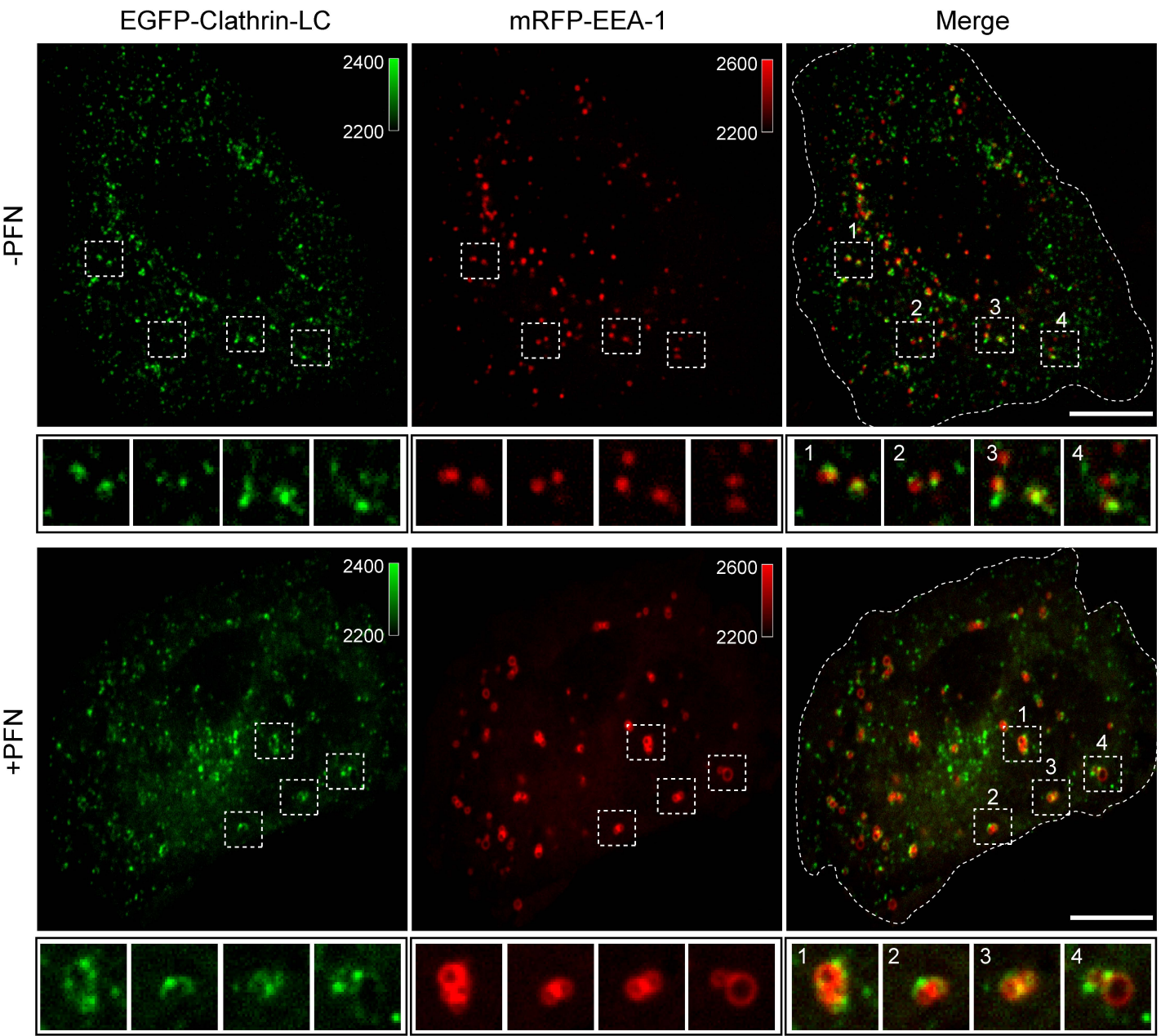
EGFP-Clathrin-LC
mRFP-EEA-1
Merge
-PFN
+PFN
2400
2200
2600
2200
1
2
3
4

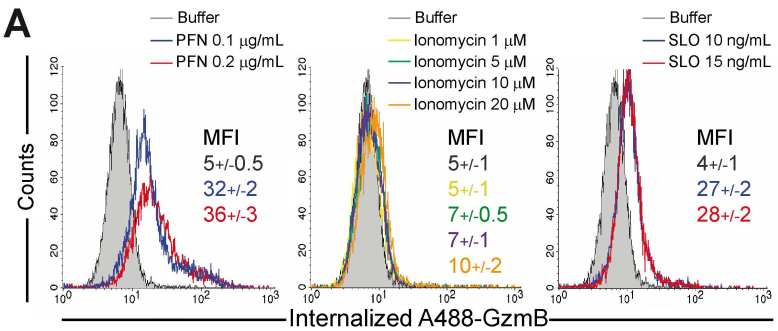
A
Buffer
PFN 0.1 μg/mL
PFN 0.2 μg/mL
MFI
5+/-0.5
32+/-2
36+/-3
Buffer
Ionomycin 1 μM
Ionomycin 5 μM
Ionomycin 10 μM
Ionomycin 20 μM
MFI
5+/-1
5+/-1
7+/-0.5
7+/-1
10+/-2
Buffer
SLO 10 ng/mL
SLO 15 ng/mL
MFI
4+/-1
27+/-2
28+/-2
Counts
Internalized A488-GzmB

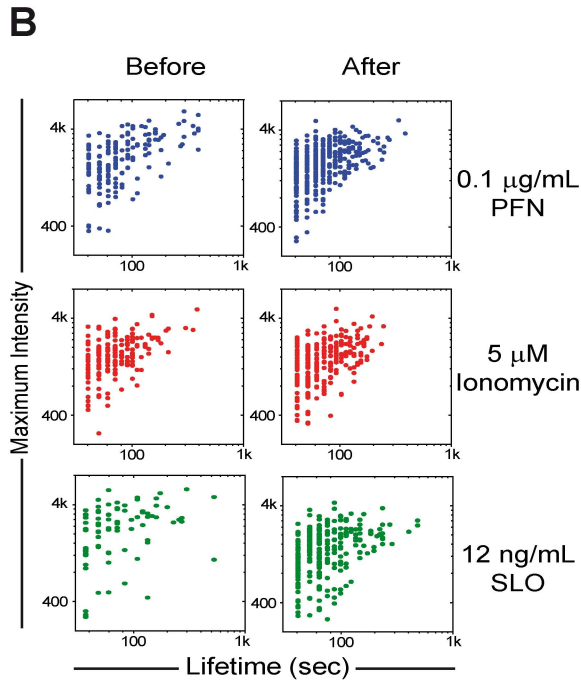
B
Before
After
0.1 μg/mL PFN
5 μM Ionomycin
12 ng/mL SLO
Maximum Intensity
Lifetime (sec)

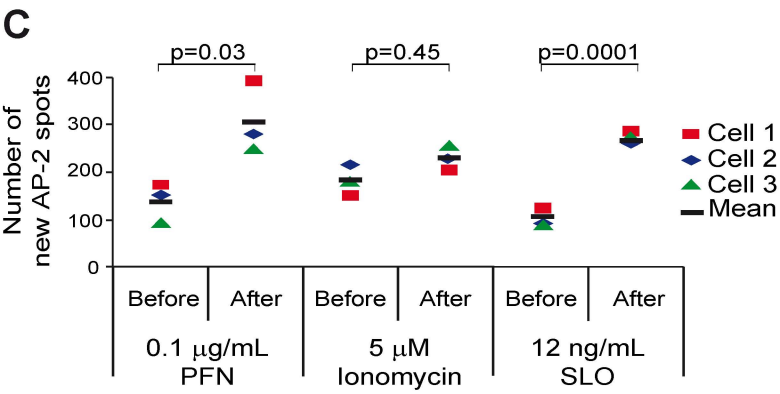
C
p=0.03
p=0.45
p=0.0001
Number of new AP-2 spots
Cell 1
Cell 2
Cell 3
Mean
Before
After
0.1 μg/mL PFN
5 μM Ionomycin
12 ng/mL SLO

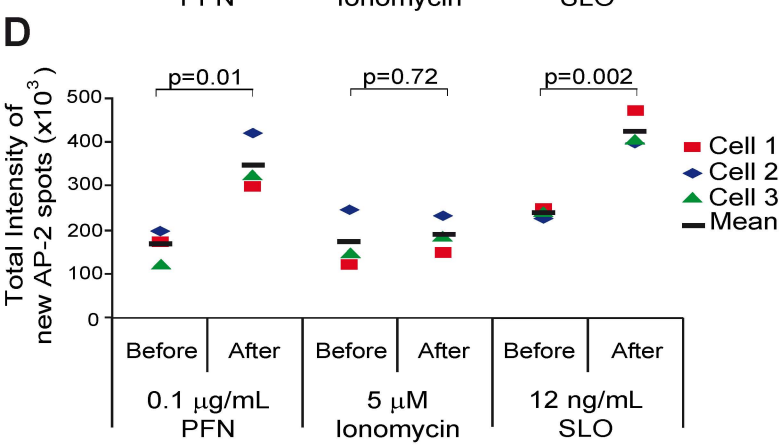
D
p=0.01
p=0.72
p=0.002
Total Intensity of new AP-2 spots (x10^3)
Cell 1
Cell 2
Cell 3
Mean
Before
After
0.1 μg/mL PFN
5 μM Ionomycin
12 ng/mL SLO

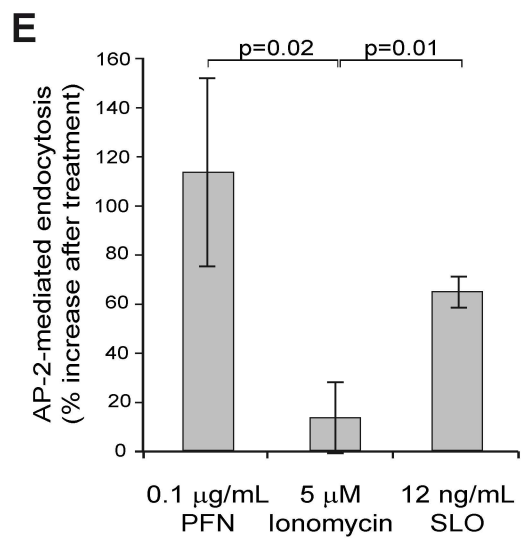
E
p=0.02
p=0.01
AP-2-mediated endocytosis (% increase after treatment)
0.1 μg/mL PFN
5 μM Ionomycin
12 ng/mL SLO

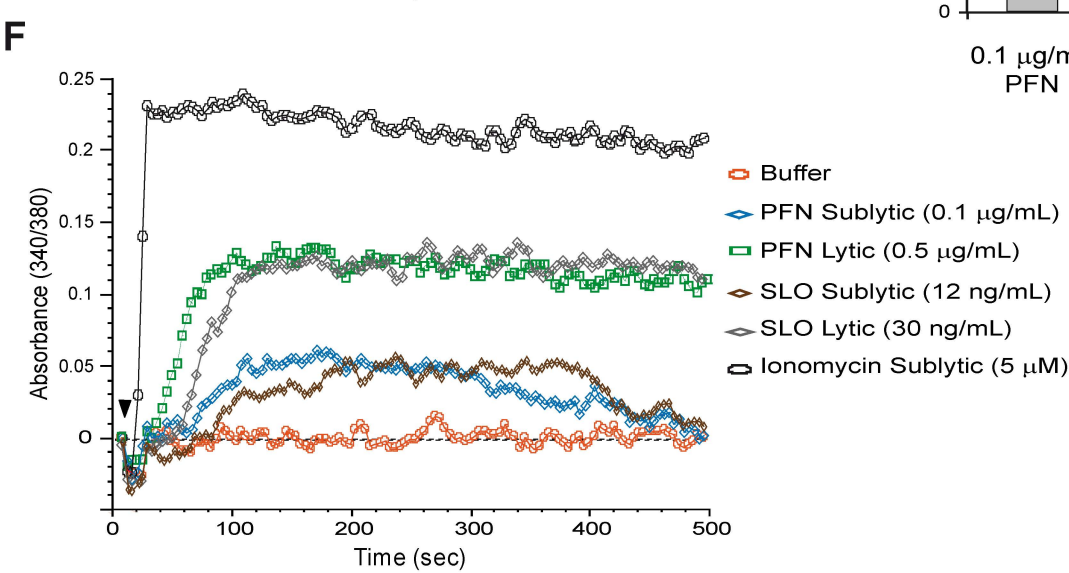
F
Absorbance (340/380)
Time (sec)
Buffer
PFN Sublytic (0.1 μg/mL)
PFN Lytic (0.5 μg/mL)
SLO Sublytic (12 ng/mL)
SLO Lytic (30 ng/mL)
Ionomycin Sublytic (5 μM)

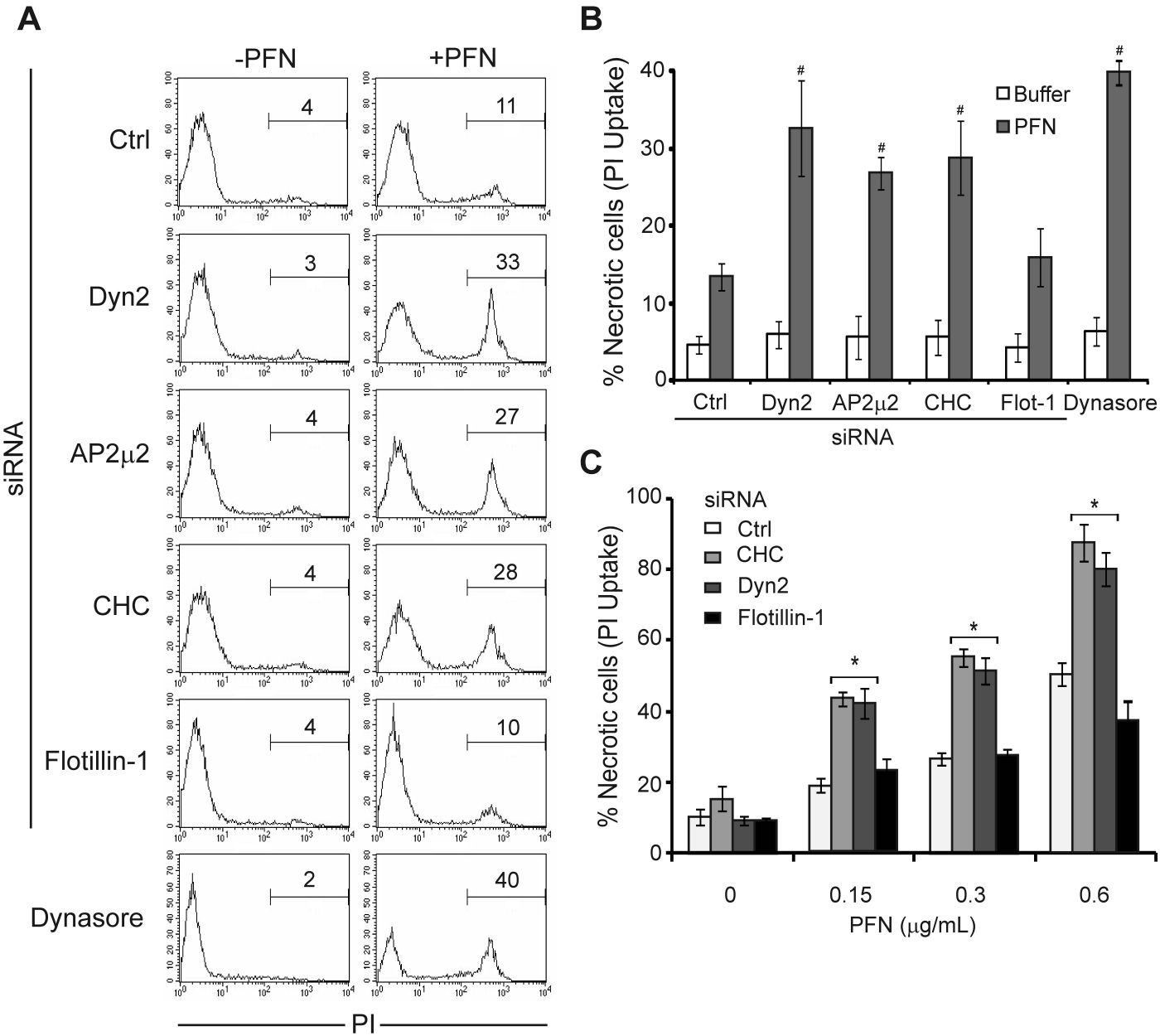
A
-PFN
+PFN
siRNA
Ctrl
Dyn2
AP2μ2
CHC
Flotillin-1
Dynasore
4
11
3
33
4
27
4
28
4
10
2
40
PI
B
% Necrotic cells (PI Uptake)
Buffer
PFN
Ctrl
Dyn2
AP2μ2
CHC
Flot-1
Dynasore
siRNA
C
% Necrotic cells (PI Uptake)
siRNA
Ctrl
CHC
Dyn2
Flotillin-1
PFN (μg/mL)

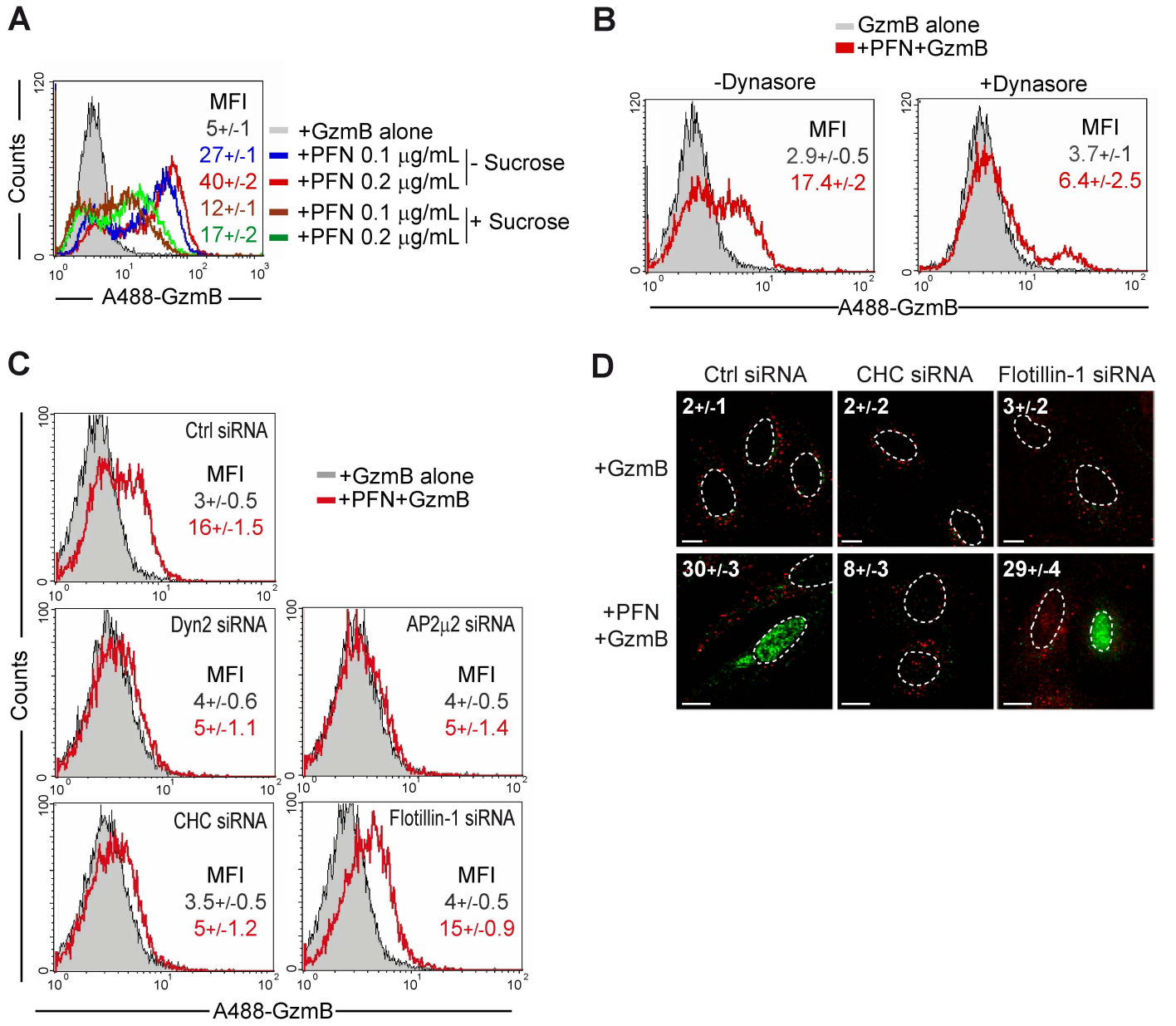
A
Counts
MFI
5+/-1
27+/-1
40+/-2
12+/-1
17+/-2
+GzmB alone
+PFN 0.1 µg/mL
+PFN 0.2 µg/mL
- Sucrose
+PFN 0.1 µg/mL
+PFN 0.2 µg/mL
+ Sucrose
A488-GzmB
B
GzmB alone
+PFN+GzmB
-Dynasore
+Dynasore
MFI
2.9+/-0.5
17.4+/-2
MFI
3.7+/-1
6.4+/-2.5
A488-GzmB
C
Counts
Ctrl siRNA
MFI
3+/-0.5
16+/-1.5
+GzmB alone
+PFN+GzmB
Dyn2 siRNA
MFI
4+/-0.6
5+/-1.1
AP2µ2 siRNA
MFI
4+/-0.5
5+/-1.4
CHC siRNA
MFI
3.5+/-0.5
5+/-1.2
Flotillin-1 siRNA
MFI
4+/-0.5
15+/-0.9
A488-GzmB
D
Ctrl siRNA
CHC siRNA
Flotillin-1 siRNA
+GzmB
+PFN
+GzmB
2+/-1
2+/-2
3+/-2
30+/-3
8+/-3
29+/-4

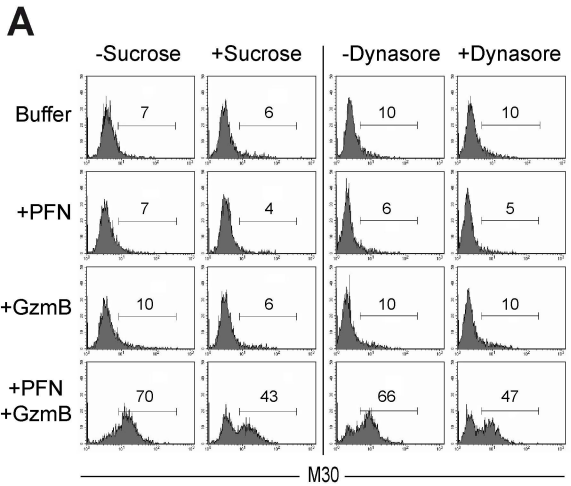
A
-Sucrose
+Sucrose
-Dynasore
+Dynasore
Buffer
+PFN
+GzmB
+PFN +GzmB
7
6
10
10
7
4
6
5
10
6
10
10
70
43
66
47
M30

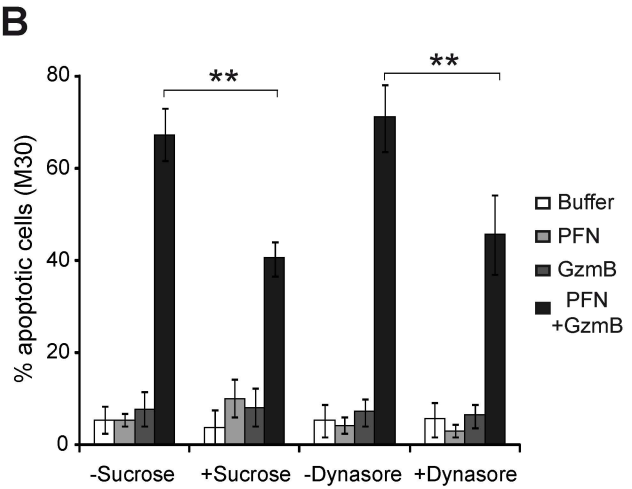
B
% apoptotic cells (M30)
80
60
40
20
0
**
**
-Sucrose
+Sucrose
-Dynasore
+Dynasore
Buffer
PFN
GzmB
PFN +GzmB

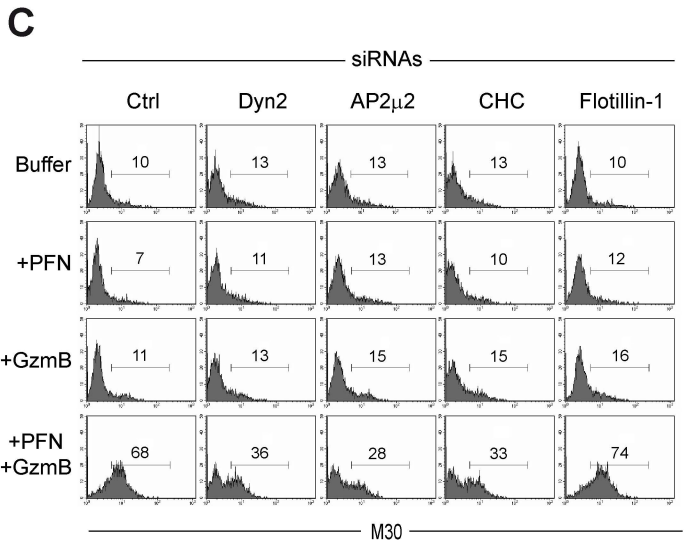
C
siRNAs
Ctrl
Dyn2
AP2μ2
CHC
Flotillin-1
Buffer
+PFN
+GzmB
+PFN +GzmB
10
13
13
13
10
7
11
13
10
12
11
13
15
15
16
68
36
28
33
74
M30

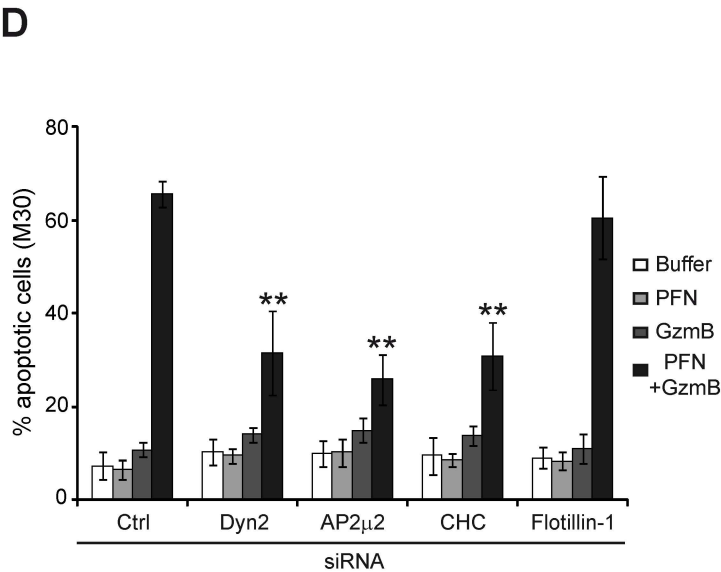
D
% apoptotic cells (M30)
80
60
40
20
0
**
**
**
Ctrl
Dyn2
AP2μ2
CHC
Flotillin-1
siRNA
Buffer
PFN
GzmB
PFN +GzmB

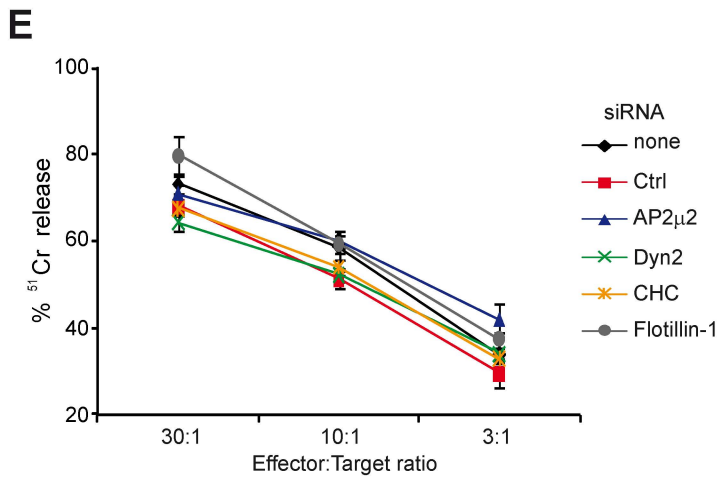
E
% 51Cr release
100
80
60
40
20
30:1
10:1
3:1
Effector:Target ratio
siRNA
none
Ctrl
AP2μ2
Dyn2
CHC
Flotillin-1